CHAPTER 20

Interactions of Polymers with Carbon Nanotubes

Rachel Yerushalmi-Rozen, Céline Bounioux

Department of Chemical Engineering, and The Ilse Katz Center for Meso and Nanoscale Science and Technology, Ben-Gurion University of the Negev, Beer Sheva, Israel

Igal Szleifer

Department of Chemistry, Purdue University, West Lafayette, IN, USA

CONTENTS

1. INTRODUCTION

Carbon nanotubes (CNTs) are cylindrical graphitic structures characterized by a typical diameter in the range of 0.8–2 nm for single-walled nanotubes (SWNTs), 10–40 nm for multi-walled nanotubes (MWNTs), and a length up to millimeters resulting in an aspect ratio (length/diameter) significantly larger than 1000. Individual SWNTs exhibit metallic or semi-conducting behavior depending on the diameter and spiral conformation (helicity) of the carbon rings [1, 2]. CNTs play a special role in current material science due to their unique high mechanical strength [3, 4], high thermal and chemical stability, and excellent heat conduction [5, 6]. The superb physical and electrical properties of CNTs result from the chemical nature of the sp^2-bonded carbon, and their nanometric diameter combined with their length.

CNTs may be thought of as rolled graphene sheets where the energy levels of the original "semi-metal", i.e. a semiconductor with a zero band gap, are modified due to the induced curvature. Distortion either increases the overlap between the conductance and valence bands, (creating a metallic SWNT) or opens a wider band-gap forming a semi-conducting SWNT [1, 5] with a band-gap that depends on the tube diameter. The semi-one-dimensional structure of SWNTs leads to ballistic transport in metallic SWNTs, enabling them to carry high currents, in the range of 10^9 A/cm^2, with essentially no heating [6]. The electronic properties of MWNTs are rather similar to those of SWNTs, due to the weak coupling between the cylinders.

ISBN: 1-58883-079-9

Chemistry of Carbon Nanotubes
Edited by V. A. Basiuk and E. V. Basiuk
Pages: 1–12

The discovery of CNTs [7] followed by the development of methods for controlled synthesis of SWNTs [8–11] has marked the emergence of the CNT era in materials science and technology. CNTs are expected to play a major role in nano-electronics where they may serve as active components in nano-switches and nano-transistors [12], electron emission sources [13,14], chemical sensors [15–16], and act as molecular wires connecting components in nano-devices [17]. CNTs were shown to be a valuable component in polymeric nano-composites [18]. Current literature suggests that CNT-based materials form a new class of lightweight super strong functional materials [19]. Applications for air and space technologies [20], energy storage [21], molecular sensors [22], and more were described.

Utilization of CNTs for the various applications described above rely on the ability to process individual tubes and disperse them in a medium, without causing damage to the tube structure or diminishing its unique properties. Yet this is a non-trivial task due to the tendency of as-synthesized SWNTs to pack into crystalline structures known as bundles or ropes that contain hundreds of well-aligned SWNTs.

The over-micron long ropes further entangle into networks rendering the carbon-powder insoluble in aqueous and organic liquids, thus making them practically unprocessable. In Figure 1 we present scanning electron microscopy micrographs of SWNT and MWNT powders.

Bundling, aggregation, and agglomeration have been identified as the major obstacles for utilization of CNTs in applications ranging from nanoelectronics to composite materials. Thus, much effort is devoted to the development of efficient methods of bundles—exfoliation into individual tubes and dispersion of the exfoliated tubes in different media [26, 27].

Over the last few years, novel strategies have been developed for exfoliation and dispersion of CNTs. The different methods belong to two distinct categories: (*i*) *highly interventional*—in this category we include methods that rely on severe to mild modification of the graphene π-system that is the origin of the high polarizability of the tubes and the origin of the strong van der Waals (vdW) attraction among them. Included are methods of chemical functionalization [28] via covalent linking of either monomers, oligomers, or polymers [29–38], complexation via π–π interactions [39, 40], and adsorption of charged surfactants [41–47]. (*ii*) *Weakly interventional*—In this approach, CNTs are decorated by weakly adsorbed or end-attached polymers that do not intervene with the electronic structure of the tubes. Weak, long-ranged entropic repulsion among the polymeric chains introduces a kinetic barrier that prevents bundling and agglomeration of CNTs and enables the dispersion of tubes in a variety of liquids and polymeric matrices.

In the following we describe in detail the problem and the role of polymers in shaping the behavior of CNTs in different media.

2. PHYSICAL CHEMISTRY OF CARBON NANOTUBES: THE INTER-TUBE INTERACTION POTENTIAL

The physical properties of materials and their phase behavior are determined by their intermolecular interactions. In complex systems, such as those involving supra-molecular structures, aggregates, or the case of interest here, CNTs; the interatomic interactions do not suffice for creating the complete physical picture of how the structures interact. A better understanding of the behavior of these species is obtained via the inter-particle interactions [48]. In the case of CNTs the interactions at the simplest level are obtained by summing over all the possible pairs of carbon atoms of the different tubes, with the proper incorporation of solvent effects.

In Figure 2 we present the inter-tube interaction potential of two individual SWNTs derived using the Girifalco model [49]. In this approach the vdW interactions between tubes are integrated over two cylindrical tubes in vacuum, ignoring specific solvent effects.

Due to the very asymmetric characteristics of SWNTs, the interaction potential is a very strong function of the angle between the tubes. Here, we focus on bundle formation and therefore relate to interactions between parallel tubes [Figure 2]. The important and interesting features of this potential are two: (*i*) a very deep attractive well found when the two CNTs are very close to contact distance, and (*ii*) the very short range of the attraction. As observed in Figure 2, the strength of the attraction reaches values of 40 times the thermal energy per nanometer of interaction. This implies a contact energy between two parallel CNTs of 1-micron length each of 40,000 the thermal energy. Clearly,

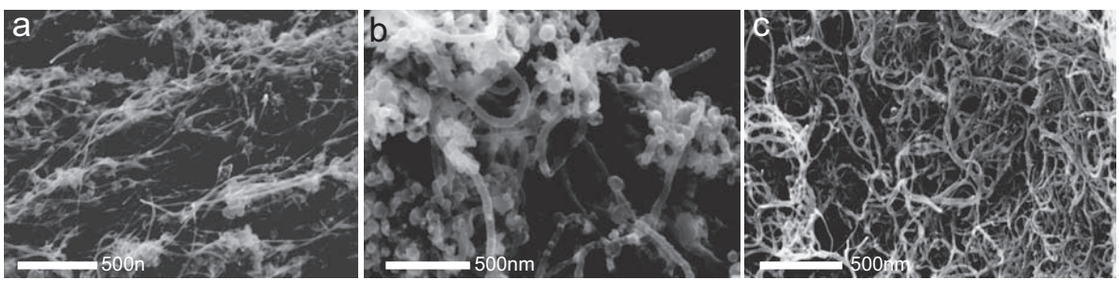

AQ9 **Figure 1.** SEM micrographs of dry (as-produced) powders of CNTs from different sources, showing bundles and ropes of SWNTs along with carbonaceous species and the catalyst [23, 24] (*a*) SWNTs synthesized via arc-discharge, (*b*) MWNTs synthesized via arc-discharge, and (*c*) SWNT synthesized via the HiPCO process [23, 25].

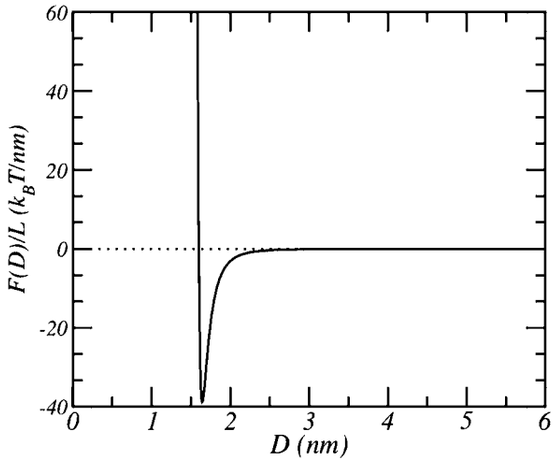

Figure 2. The specific interaction potential between two parallel SWNTs as a function of the distance between them [27, 50].

tubes will tend to bundle, as experimentally observed [1–3, 9]. The range of the attractive interaction is only a couple of nanometers, as the interaction has a value of less than k_BT at a separation between the centers of tubes of less than 2.5 nm. The short range of the attractive potential is the key for the use of polymers for exfoliating and dispersing SWNTs, as explained below.

It is interesting at this point to make a distinction between CNTs and colloidal particles. The vdW interactions between particles have a typical range of a few molecular diameters and the strength of the attraction is proportional to the particles' size. In the case of colloidal particles, the relevant size-scale is in the micron range and therefore typical vdW attractions are long-ranged compared to any typical molecular length scale, and very strong. On the other hand, CNTs have one dimension that is nanometric and therefore the range of the interactions is relatively short (as shown in Figure 2), while the other dimension is very large, making the total strength of the interaction very large. These differences in the range of the interactions can serve to design surface modifiers that impose steric repulsions at relatively short distances from the surface in such a way that there are enough to stabilize CNTs, but will not be of enough range to properly stabilize colloidal particles [27, 50, 51, 52].

AQ1

To summarize this point, the range of the attractive vdW interactions between particles is determined by the dimensions and geometry of the particles. In general, the interaction range is a few times the particle size. Classical colloids are mesoscopic objects and are dominated, in general, by long-ranged dispersive forces. On the other hand, fullerenes [53] and SWNTs are hollow structures with two (SWNTs) or three (fullerenes) nanometric dimensions. Thus, they interact via a short-ranged intermolecular potential that characterizes large molecules rather than small colloids [27, 51].

AQ2

Here we note that the attractive, short ranged interaction between CNTs is large when compared to either atoms or colloidal particles, and results from the high polarizability of the graphene π-system along the tubes [50, 54]. Furthermore, due to the specific geometry of the tubes, the interactions are expected to be very strong when the CNTs are parallel to each other. However, when oriented perpendicular to each other, the vdW attractions should have a character very similar to that of any polyatomic molecule, expected to be only a few times the thermal energy, and still short ranged. Thus, inter-tube interactions of CNTs depend strongly on the fact that two dimensions are nanoscopic, and the third is mesoscopic, giving rise to the special range, magnitude, and angular dependence of the interactions.

3. EXFOLIATING AND DISPERSING CARBON NANOTUBES–THE APPROACH

Going back to the methods used for exfoliation and dispersion of SWNTs, we can now state that the *highly interventional* approaches aim to reduce the depth of the attractive minima in the effective inter-tube potential. To achieve that, covalent interactions are invoked as sp^3-bonding results in localization of the π electrons [54], thus reducing the polarizability of the tubes and consequentially the vdW attraction between adjacent tubes. Alternatively, specific interactions of a strength similar to that of the tube cohesion energy may be invoked as was suggested, for example, by Blau et al. [56].

The *weakly interventional* approach is essentially different, as it aims at introducing weak (of order of a few k_BT) repulsions at a large inter-tube distance [27, 57–59]. This approach takes advantage of the short range of the attraction acting between SWNTs. By invoking, for example, an osmotic (steric) repulsion among tails of tethered copolymers, in good solvent conditions [60], it is possible to prevent aggregation, bundling, and agglomeration of CNTs in liquid media as demonstrated in Figure 3.

A sensitive measure of the interaction between the dispersing agent and SWNTs is provided by spectroscopy. In Figure 4 we present UV-Vis spectra of SWNTs dispersed in

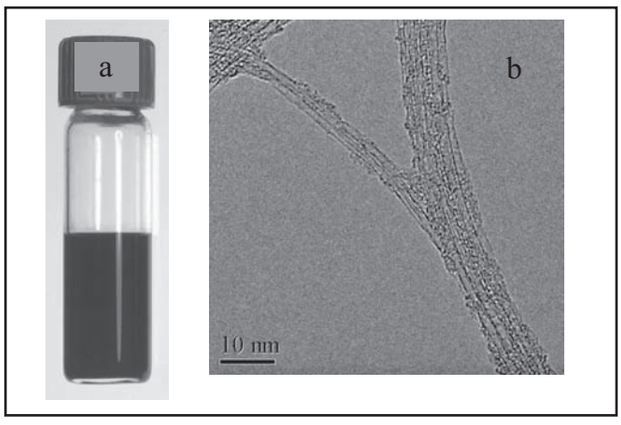

Figure 3. (*a*) An optical image of a SWNT dispersion in a block copolymer solution [51, 58, 59] and (*b*) a TEM image of a bundle of SWNTs going through exfoliation. The sample was obtained by drying a droplet of a SWNT dispersion as in (*a*).

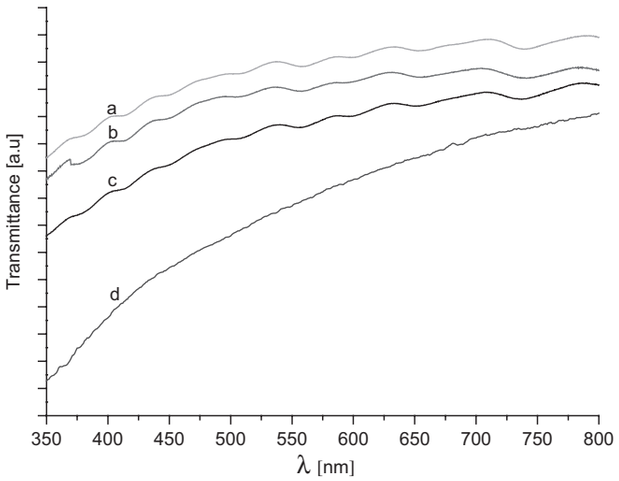

Figure 4. UV-Vis absorption spectra of SWNTs (HiPco [25]) in (*a*) toluene (*b*) aqueous dispersion of Plurincs (P123, 1 wt.%). (*c*) Toluene dispersion in a block copolymer PS-PMAA [62]. (*d*) Chemically modified SWNT (HiPco), Reprinted with permission from Ref. [61], Wagner et al. In *Polymeric Stabilization of Colloidal Dispersions.* Napper, D. H., ed. Orlando: FL: Academic Press, Inc., (1993).

toluene [Figure 4(a)], in solutions of a block of copolymers [Figure 4 (b and c)], and for comparison, spectra of chemically modified SWNTs [63]. Theoretical modelling [1] suggests that the molecular-like structure of CNTs and the confinement in the circumferential direction lead to the clearly recognized van Hove singularities in the optical absorption UV-Vis spectra of the dispersed SWNTz, as indeed observed in the step-like structure seen in Figure 4(a). Note that the effect of block-copolymer adsorption is very different from the case of chemical functionalization [Figure 4(d)], where strong, covalent interactions lead to localization of the π-electrons as indicated by smoothing of the absorption spectra and the disappearance of the step-like structure.

4. POLYMER-INDUCED STERIC STABILIZATION OF CARBON NANOTUBE DISPERSIONS

Among the more efficient steric stabilizers are block-copolymers and end-functionalized polymers [Figure 2(a)].

Block copolymers are comprised of covalently bonded, chemically distinct, and often mutually incompatible moieties (designated A-B and A-B-A for di-blocks and tri-blocks, respectively, [Figure 5] [64].

In a selective solvent that is a "good solvent" for one of the blocks (A) and a "poor solvent" for the other (B) [60], the less soluble block may adsorb to the CNT surface while the other dangles into the solution, as shown in the simulation snapshot presented in Figure 6. At high enough surface coverage the tethered polymers will form a "polymer brush" [65, 68, 69], in which the chains are stretched away from the surface and form a steric barrier that prevents other polymer-decorated CNTs from approaching.

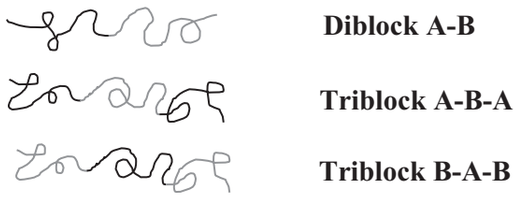

Figure 5. Schematic representation of different types of block copolymers.

To quantify the effect of steric repulsion, we have used a molecular theory that enables the calculation of the structural and thermodynamic properties of polymers attached to surfaces. For the particular application to nanotubes see refs. [27, 51, 69]. We look at the structure of polymer molecules end-tethered to form a nanotube surface at a finite coverage. Figure 7 shows polymer density profiles for two parallel CNTs at various separations. AQ3

Figure 7(A) is for a relatively large separation and the distribution of polymer segments around the CNT is symmetric. Note that the *x* and *y* axes have different scales. As the distance between the CNTs decreases one can see that there is an increase in the density of the polymers in the

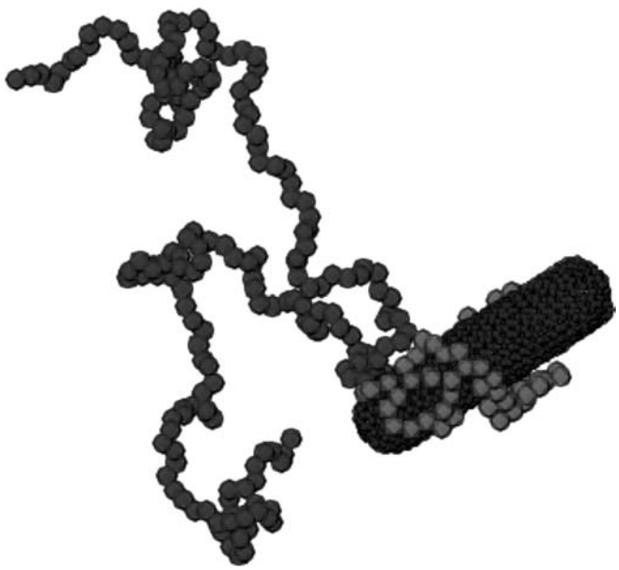

Figure 6. Snapshot from a molecular dynamics simulation of a triblock copolymer PEO-PPO-PEO (A-B-A) and a carbon nanotube. The *red spheres* represent PO (hydrophobic, B) segments, while the *blue spheres* represent the hydrophilic EO (A) segments. The simulations were carried out using the coarse grained model for the polymer derived from atomistic simulations in ref. [65]. The snapshot shown is from a long run with an initial condition in which the CNT and the polymer are very far from each other. The particular configuration shown is characteristic and shows all the PO segments adsorbed on the CNT while the hydrophilic EO segments preferred to extend towards the water. Note the lack of order in the adsorbed PO chain. At a finite number of triblocks, the simulations show multiple adsorption of polymer molecules by the PPO block and the formation of a 'brush" from the PEO blocks [67].

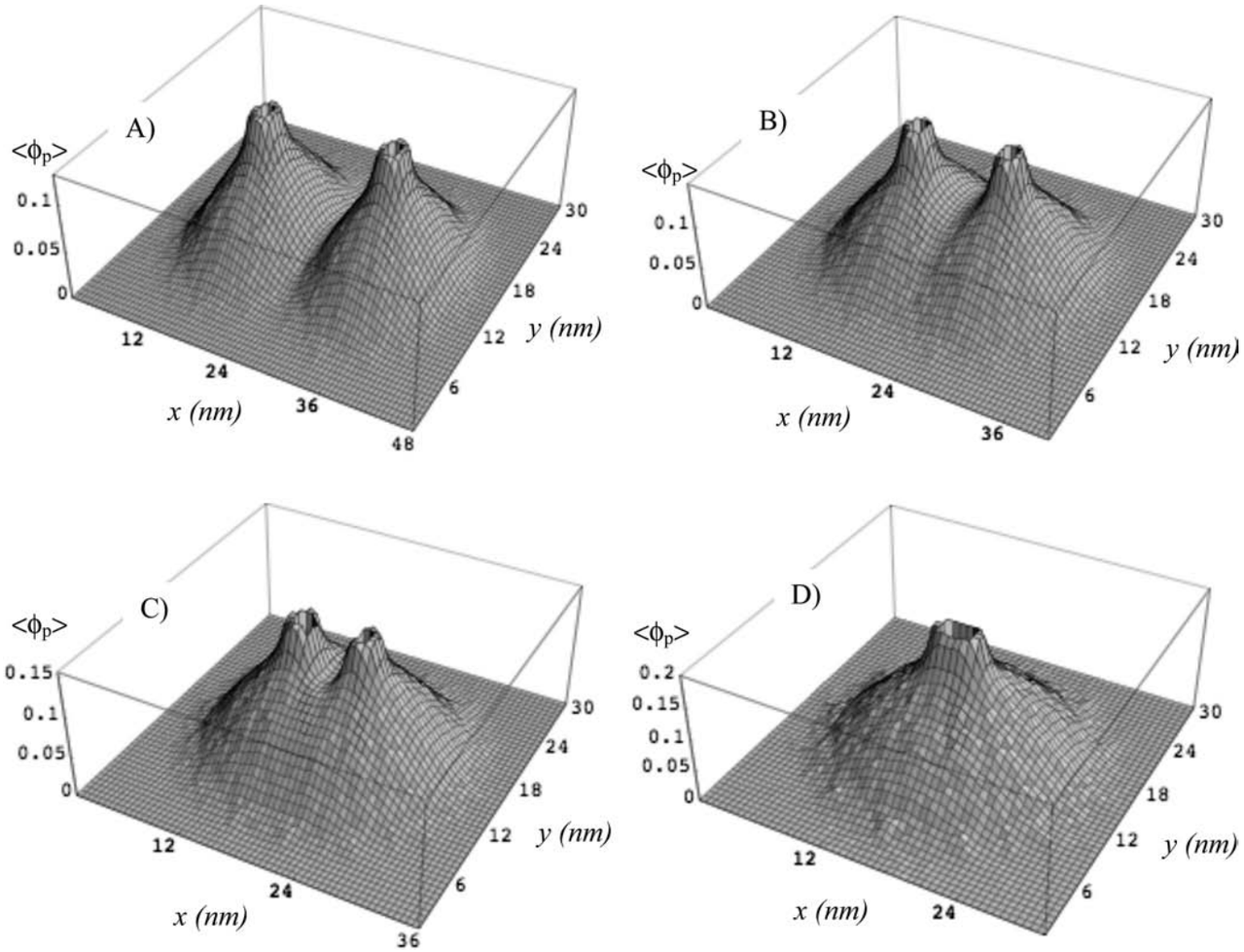

Figure 7. The polymer volume fraction, in the plane perpendicular to the CNT, as a function of the distance (nm) from the center of two parallel tubes. The distances between the centers of the CNTs are: (*A*) D = 14 nm, (*B*) D = 9 nm, (*C*) D = 5 nm and (*D*) D = 1.2 nm All cases correspond to polymers with 100 EO segments and the polymer line density is 2 nm^{-1}. Note that the *x* scale is different for the four cases.

back part of the tubes. This is due to the steric repulsions between the polymer chains. The largest effect is observed when the tubes are in contact [Figure 7(D)]. The steric repulsions between the polymers and the change in conformational entropy associated with the loss of space due to the presence of the other tube results in an effective repulsive interaction that is measured by the free energy per unit length of the parallel polymer-coated CNT as a function of their separation.

The effective repulsions are shown in Figure 8 for two different polymer chain lengths. One can see that as the SWNTs get closer, the repulsion increases and the longer the chain, the longer range and stronger the repulsive interactions. We have also shown that the strength of the repulsions increases with surface coverage [27, 51].

Two interesting results may be deduced from Figure 8. First, the interactions at contact are highly repulsive but finite. This is a direct consequence of the geometry and dimensions of the tubes. For planar surfaces, the repulsive interactions diverge [27, 69]. Second, in the region that is

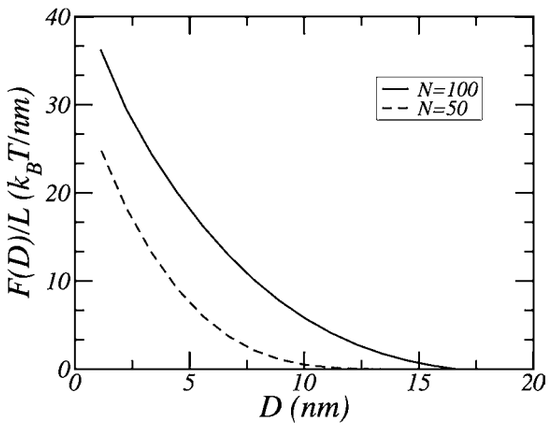

Figure 8. Repulsive interactions between parallel CNTs coated with end-tethered polymers as a function of the distance between the CNT centers. The two curves represent different polymer chain lengths. The polymer line density is 3.3 nm^{-1}.

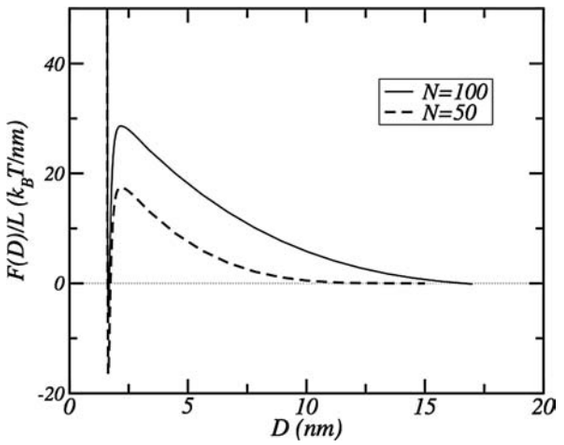

Figure 9. The total interaction potential between parallel CNTs with end-grafted polymers. The potentials are obtained by adding the vdW attractive contribution [Figure 3], and the steric repulsions arising from the tethered polymers [Figure 7]. The conditions are as in Figure 7.

relevant for exfoliation of SWNT bundles, we see the presence of a large repulsion for both chain lengths. For example, at D = 5 nm, there are no attractions [see Figure 2], but there is a strong repulsion [see Figure 8] suggesting a large steric barrier between the tubes.

To see the total potential we add the attractive part from Figure 2 to the steric repulsions shown in Figure 8, the result is shown in Figure 9. While the attractive component of the interaction is still present, the tubes would have to cross a very high barrier to reach that minimum. The steric barrier is many times the thermal energy and therefore dispersed SWNTs do not have enough available energy to reach that state.

The practical way to achieve CNT dispersion is to sonicate the CNT powder in a block-copolymer solution leading to exfoliation of the tubes, followed by adsorption of the block copolymer through the insoluble block [Figure 6], and formation of a tethered layer of the soluble block that presents a steric barrier, which stabilizes the individual CNT in solution.

5. STERIC STABILIZATION–THE MICROSCOPIC MODEL

The polymer configuration presented in Figure 6 is very different from what is known as "polymer wrapping". In the latter model, first suggested for synthetic, non-conjugated polymers by O'Connell et al. [70], polymer wrapping of individual CNTs is believed to result in screening of the hydrophobic interaction at the CNT-water interface, leading to dispersion of individual tubes in aqueous solutions. Yet this rationale is questionable, as numerous studies clearly show that the hydration force acting between CNTs in water is similar to the force acting between CNTs in vacuum, suggesting that bundling is dominated by the vdW attraction between the CNTs rather than by the hydrophobic interaction. In this scenario, polymer wrapping cannot diminish the vdW attraction to a low enough value, and thus cannot be the dominant mechanism in CNT dispersion.

Different scenarios of CNT wrapping by polymers were observed in systems where the driving force for CNT-wrapping is provided by chemical interactions between the π-system of the CNT and the functional groups comprising the polymers. Here, wrapping results from electrostatic interactions, π-stacking, or hydrogen bonding. It is now well accepted that polymer-wrapped CNTs are strongly associating, tightly bound systems where the tube surface chemistry, electronic structure, and the intrinsic inter-tube interactions are modified by the wrapping. Among the wrapping polymers are biopolymers, such as DNA and peptides [71–77], and conjugated polymers [78–82].

It is interesting to note that the computer simulation results presented in Figure 6 suggest that the insoluble block adsorbs on the nanotube but does not wrap it. Rather, the polymer forms a disorganized layer that achieves optimal CNT-insoluble block interactions but still allows for some conformational entropy of the adsorbed chain.

Experimental investigation of the structure of CNT dispersions has been carried out by scattering methods [83–85]. Due to their cylindrical structure and high aspect ratio, dispersed SWNTs are expected to exhibit a characteristic -1 power-law dependence of the scattering intensity on the scattering angle. Yet, in most of the studies the observed exponent is closer to -2. A possible explanation for the observed discrepancy was discussed by Dror et al. [86]. In a detailed study using Small-Angle–Neutron scattering, they found that polymer-decorated CNTs, in a sterically stabilized dispersion, form structures where a thin core (of typically less than 4 tubes) is surrounded by a thick corona of swollen coils (15–17 nm). These parameters suggest that the dispersing polymer retains its solution coil-like structure with typical dimensions that characterize polymers in good-solvent conditions. The model presented above relates to brush-like structures formed by physical adsorption of block-copolymers onto CNTs. Over the last few years it was suggested that at higher block-copolymer concentrations, micelles might play an important role in the dispersion mechanism [87, 88].

The structure of polymer-dispersed CNTs is just starting to emerge. Comprehensive studies combining experimental and theoretical approaches are needed in order to elucidate the detailed structure of polymer-decorated CNTs and their behavior in solution.

6. THE ROLE OF SPECIFIC CHEMICAL INTERACTIONS IN STERIC STABILIZATION

So far, we have focused on the (soluble) A-block, and have shown that physical, non-specific interactions are the origin of the repulsive barrier introduced into the effective pair potential. Yet the strategy presented here relies on the anchoring ability of the B block. On the one hand, the attractive interaction per segment should be small, so as to minimize the effect on the electronic structure of the

polymer-decorated CNT. However, the overall tethering energy pair chain should exceed k_BT to ensure irreversible tethering. Here, one may take advantage of the polymeric nature of the B block, where an effective anchoring energy of a few k_BT may be achieved due to the large number of weakly attached monomers. The tethering energy per monomer is then determined by the specific interactions between the B block and the CNT. The B block will adsorb on the surface of the CNT when the net attractive interaction between a polymer segment and the surface is higher than the interaction between the solvent and the surface. We can define the surface effective attraction by AQ4 $\chi_{ps} = (U_{sol-sur} - U_{pol-sur})/K_BT$ where $U_{i\text{-}sur}$, i = polymer or solvent, represents the attraction between species, i, and the surface. Note that a positive value of χ_{ps} means an attraction for the polymer. In reality, each of the U terms is a difference between the attraction of a given species to its own type of molecules and the surface. Therefore, the specific chemical nature of the adsorbing block and the solvent will determine the strength of the polymer-surface interaction, χ_{ps}, that in turn, together with the polymer chain length, will determine the amount of adsorbed polymer. It is also important that the soluble block has a smaller χ_{ps} value than that of the insoluble block, otherwise competitive adsorption of the two blocks may take place. The specific details of the chemical nature of the solvent and the two blocks can be used as an important tool for engineering the surface behavior of CNTs, as it allows one to tune the adsorbed amount and thus provides control over the strength and range of the steric barrier formed by the soluble block.

The simulations snapshot shown in Figure 6 corresponds to a polymer-surface interaction $\chi_{ps} \cong 0.9$ for the insoluble block (B). This relatively large value was estimated from the available atomistic simulations for PO [66]. The value for the A (soluble) block is on the order $\chi_{ps} \cong 0.65$. Therefore, the effective gain by adsorbing a PO segment is 0.25 k_BT. The large PO-CNT attraction results in adsorption of all the PO segments. Even in this case, the adsorbed polymer adopts a random configuration allowing the PPO block to optimize its free energy by on the one hand maximizing the vdW interactions with the surface, and at the same time maximizing the entropical configuration of the adsorbed segments.

7. USING BLOCK COPOLYMERS FOR PREPARATION OF CARBON NANOTUBE-BASED COMPOSITES

The approach presented here can be extended beyond preparation of stable dispersions of CNTs to the preparation of CNT-polymer nano-composites. Indeed, much effort has been devoted over the last decade to the development of polymer-based CNT composites [2]. The motivation results from the understanding that CNT-based composites may exhibit improved structural and functional properties for a vast range of applications. An important observation is that the extremely high aspect ratio of CNTs should result in a low percolation threshold [89, 90]. In the case of a non-conducting polymer matrix, percolation of CNTs is marked by a sharp increase in the electrical conductivity as a function of CNT concentration; resulting in composites that are useful for antistatic shielding, shielding of electromagnetic interference, and preparation of semi-transparent conductors [91].

As was observed in many studies, the electrical conductivity of CNT-polymer composites increases significantly (7–8 orders of magnitude) at SWNT concentrations below 0.1 wt.%. [92–96]. In addition, improved mechanical strength was measured [63, 93, 94] suggesting that the connected network simultaneously provides a mechanical backbone and a pathway for electrical conductivity.

While of great promise, a survey of current literature indicates that most of the studies of CNT-polymer composites focus on devising a method for dispersing a given type of CNT in a specific polymer matrix. Thus, different procedures have been developed for different target matrices. Yet to fulfill the technological promise of CNT-based plastics, it is necessary to develop generic methods for integration of CNTs into a variety of polymeric matrices. Furthermore, the tendency of the plastics and paint industry to adopt CNTs as fillers in mass production of polymeric commodities depends strongly on the ability of using existing composite technologies.

Here again, block-copolymers may become useful. Block-copolymers have long been used by the plastics industry as coupling agents and adhesion promoters [64, 97], significantly improving the properties of filled polymers. In the case of CNTs, the dispersing agents may be utilized to play multiple roles, acting simultaneously as dispersing agents, compatibilizers, and coupling agents for CNTs in polymeric matrices.

In this scenario, the chemical nature of the dispersing block-copolymer plays an important role: in each case the (dispersing) block copolymer should be selected so as to have one block identical (or chemically compatible) with the target matrix in order to improve the dispersibility of the exfoliated tubes in the polymer matrix.

In the following we describe the approach, discuss the inherent difficulties, and outline some of the open questions. Figure 10 details the preparation of CNT-polymer composites, using block-copolymers.

Optical image of CNT-polymer composites are presented in Figure 11 (a and b). The light-grey and semi-transparent samples are macroscopically homogeneous, flexible, and optically smooth. High resolution scanning electron microscopy was used for imaging an inner surface of the composites. In Figure 12(c), we present an image of a surface obtained by cleaving a sample of a composite. In the image one may observe (white arrow) that the SWNTs are stitching the polymer matrix, and seem to be well embedded in it. The diameter of the threads suggests that these are small bundles each composed of less than 5–10 SWNTs.

The electrical properties of the composites were characterized by dc volume conductivity measurements. The volume conductivity of different composites as a function of the SWNT weight percent [Figure 12] shows the electrical behavior expected from a composite; up to the percolation threshold the bulk conductivity increases slowly with the conductive filler weight fraction. An abrupt increase (in the

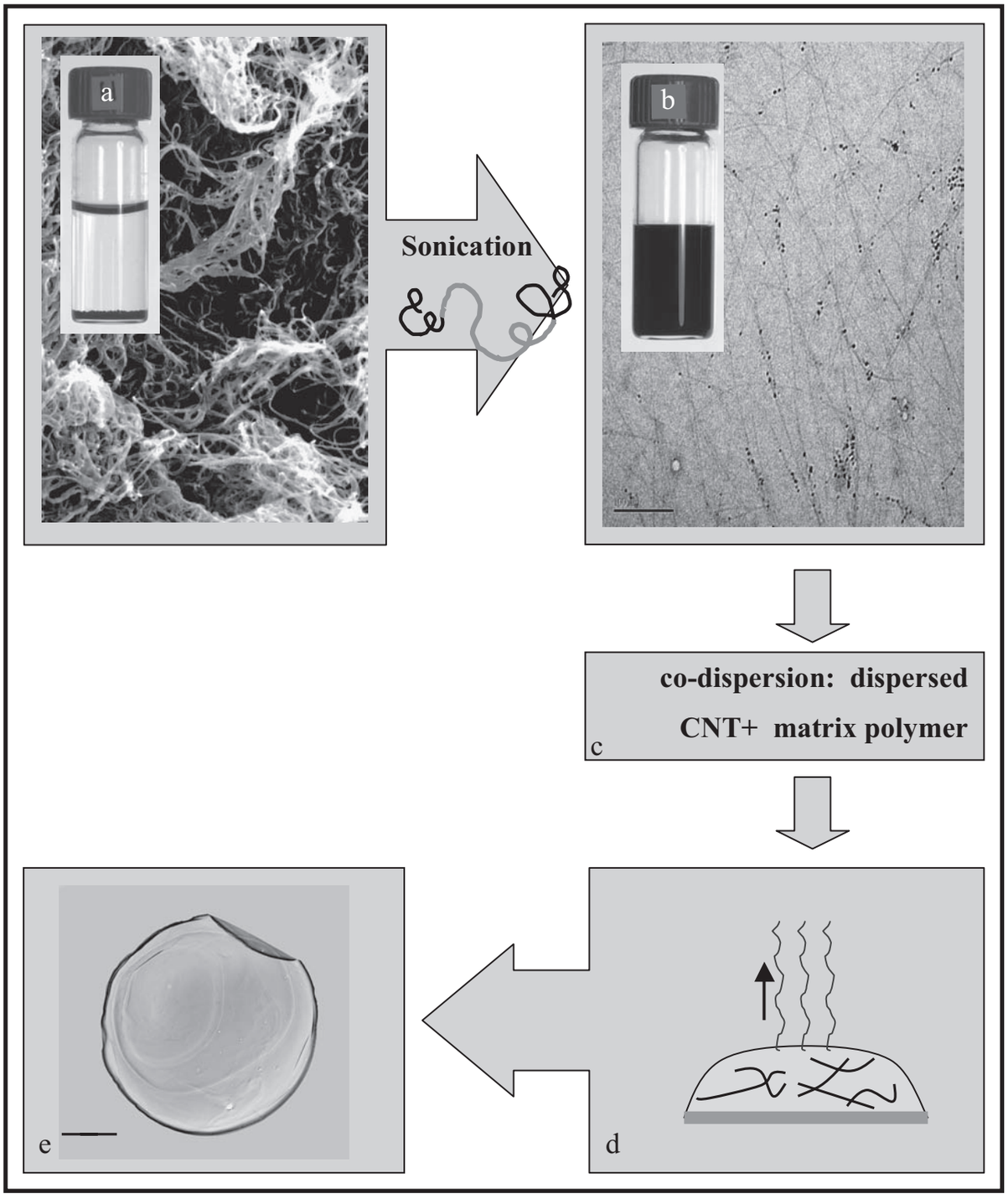

Figure 10. Schematics outlining the preparation of CNT-polymer composites (*a*) SEM image of a powder of as-prepared pristine SWNTs. Sonication of the powder in water does not lead to dispersion of the CNT (see the bottle with the CNT powder precipitated at the bottom), while mild sonication (50 W, 43 kHz, 40 min, at room temperature) of the SWNT powder in a solution of a block-copolymer (using a selective solvent) [60] leads to exfoliation of the tubes and formation of a stable dispersion of individual tubes as indicated macroscopically by the formation of a black, ink-like dispersion (*b*) and by the Cryo-TEM [58, 24] image of the vitrified dispersion (scale bars 100nm). Preparation of a CNT-polymer composite is initiated by co-sonication of the matrix polymer with the dispersed CNT (*c*) followed by poring of the mixture into a mold and drying (*e*) to form a CNT-polymer composite of desired CNT-concentration (Scale bar 1 cm). In the text we elude to four different composites: Acronal 290D where Gum Arabic (GA) served as the dispersing agent and the solvent was water, Primal 928 and Acronal 290D where Pluronic P123 tri-block copolymer was used to disperse CNT in aqueous solutions, and polydimethylsiloxane (PDMS) where Poly (ethyleneoxide-b-polydimethylsiloxane-b-ethyleneoxide) tri-block copolymer, PEO-PDMS-PEO was used in heptane. (Experimental details are described in reference [96]).

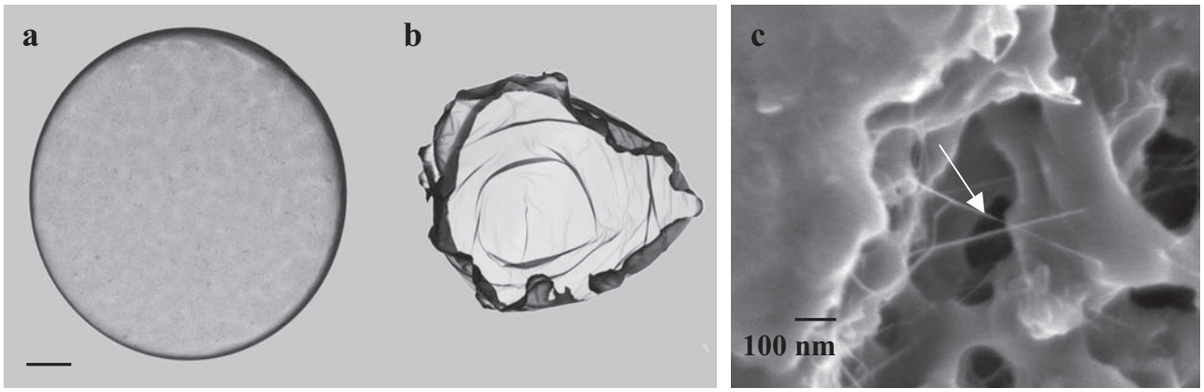

Figure 11. Optical images of CNT-polymer samples (*a*) Primal 928-P123-MWNT (MWNT concentration 0.8 wt%), (*b*) Polyacylamide-P123-SWNT (SWNT concentration 0.07 wt%), bar 1 cm, and (*c*) high resolution SEM image of Acronal 290D-GA-SWNT (SWNT concentration is 2 wt.%) [96].

order of 6–8 orders of magnitude) obtained at a wt.% < 0.1 (for SWNTs) marks the percolation threshold, and is followed by a weak increase in conductivity. This behavior, which is attributed to the establishment of multiple conducting pathways above percolation, is classical and produces the typical S-curve behavior [89–95].

Further inspection of the data presented in Figure 12 suggests that the volume conductivity of the polymer-SWNT composites depends both on the matrix and the dispersing agent. The value of the percolation threshold and the nature of the jump in the conductivity vary with the dispersing polymer and the matrix, while the PDMS and Primal matrices [Figure 12] show an abrupt jump, and the conductivity keeps increasing above the percolation threshold. The Acronal matrix (with two different dispersing agents) shows a more gradual change at the transition, and conductivity does not increase above the percolation threshold.

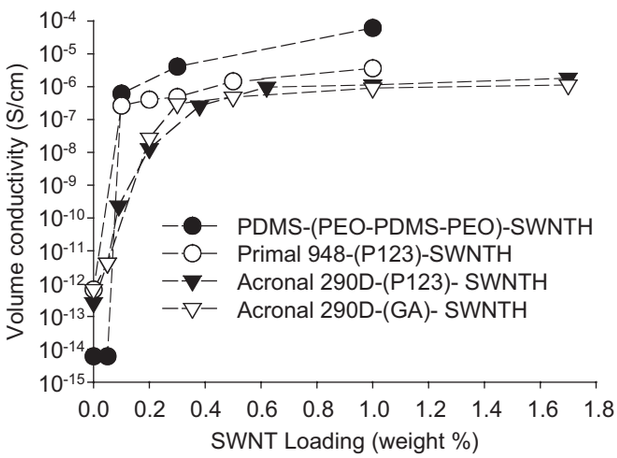

Figure 12. Volume conductivity of SWNT- polymer composites as a function of SWNT concentration in different polymeric matrices, and different dispersing polymer [96].

The origin of the observed behavior and specifically the dependence of the electrical behavior on the interfacial interactions at the CNT-polymer interface are not well understood. While many studies focus on the preparation and characterization of the physical properties of the CNT-polymer composites, the structure and the microscopic properties of the network formed by SWNTs within a polymeric matrix are not well understood. Fundamental questions related to the conductance mechanism, the topological characteristics of the network, and percolation threshold are yet to be resolved. Here, we highlight a few points. It is common to describe CNTs in polymeric matrices as non-interacting cylinders and assume that they adopt a random orientational distribution. Yet, it is often found that the networks do not exhibit a universal behavior, that the conductivity of MWNTs and SWNTs is similar above the percolation threshold, and that the percolation threshold is higher than expected from geometrical considerations [79, 99–104]. A few relevant questions are then whether the network is formed by individual nanotubes or by small clusters that percolate above a certain bulk concentration of either SWNTs or MWNTs. In the latter case, the aspect ratio of the individual moiety is expected to be less important than assumed. Another question is related to the role of tube-tube contacts in the presence of the polymer. Here, both the orientational distribution of the tubes and the behavior of the polymer at the contact points between tubes become relevant. The effect of the orientational distribution on the percolation behavior of CNTs was recently investigated in different model systems [90, 105]. It was suggested that non-random orientational distribution, such as that resulting from non-random intermolecular interactions, should affect the percolation threshold and the structure of the resulting network. Similar considerations may apply to block-copolymer decorated tubes in a selective solvent. Indeed, as was discussed above, interactions between polymer-decorated CNTs in a selective solvent that is a good solvent for the A-block are highly non-random with respect to the relative orientation of the tubes. While parallel tubes interact via a strong repulsion, tubes that orient perpendicular to each other are able to form a molecular

contact. The latter is a direct consequence of the nanometric dimensions of the tubes. As the diameter of the tubes is smaller than the typical dimensions of the polymer coil, the solvated block is able to move away from the junction formed between two crossed cylinders, thus minimizing the steric repulsion [51]. It is then reasonable to assume that the probability of junction formation would determine the percolation threshold in this system.

While these considerations are relevant for composites formed via a fast quench of a polymer dispersion, composites may be prepared via a slow process of solvent evaporation where the system is allowed to equilibrate while the solvent is evaporated. In this case, gradual evaporation of the solvent increases the concentration of the free polymer to above the semi-dilute [61] concentration and finally to the concentrated regime. In this case the steric repulsion between tails of polymers adsorbed onto CNTs is reduced, leading to re-orientation of the aggregating CNTs and formation of a different type of a network. The changes in the interactions between the polymer-coated CNTs by changing the solvent from low—molecular-weight to polymeric is significant. Here again the role of the surface geometry and the nanometric diameter of the tube play a key role in keeping the steric interactions repulsive under all conditions. However, the strength of the repulsions decreases as the molecular weight of the solvent increases. This is due to the reduction in the osmotic pressure associated with the steric repulsion as the molecular weight of the matrix increases. It is a challenging and important unsolved problem to estimate the strength of the repulsions as the solvent changes and how those interactions depend upon the type of polymer matrix.

To summarize this topic, we note that block-copolymers offer a simple, generic route for preparation of CNT-polymer composites characterized by low percolation thresholds, that may be obtained by optimizing the interfacial interactions at the CNT-polymer interface. Improved compatibility induced by the block-copolymer results in an effective higher aspect ratio as individual tubes and small bundles are dispersed in the matrix rather than large aggregates. The ability of incorporating CNTs into a given polymeric matrix by selecting a dispersing agent (the block-copolymer), which is compatible with the target matrix, is the key to this approach.

A variety of block-copolymers comprising different functional groups are currently used by the plastics industry, either as off-the-shelf products or via reliable synthetic routes [97, 106].

Chemical modification of a selected block enables the preparation of a variety of polymers (including functional groups such as styrene/diene, fluorinated moieties, mathacrylates and more) with a vast range of properties. Thus, it is possible to design and prepare a variety of composites, via the generic pathway described here, to meet different practical needs.

8. CONCLUSIONS

Over the last few years polymers have been utilized for interfacial engineering of SWNTs and MWNTs in condensed media. It has been recognized that polymers enable the incorporation of CNTs into aqueous and organic liquids, solutions, polymer melts, gels, and amorphous and crystalline matrices, opening new routes for their utilization in a variety of applications. An important observation is that polymers offer a unique tool for modification of the phase behavior of CNTs without damaging the unique properties of the individual tube.

Understanding of CNT-polymer interactions is beginning to emerge, yet a substantial effort is still required for improving our understanding of the detailed nature of interactions. Improved understanding is expected to improve our ability to tune the CNT behavior and utilize them for a variety of applications and emerging technologies.

ACKNOWLEDGEMENTS

We thank Mr. Dongsheng Zhang for the simulation snapshot presented in Figure 6. R. Y-R would like to thank the ISRAEL SCIENCE FOUNDATION, (grant No.512/06). I. S. acknowledges partial financial support from the National Science Foundation of the United States through grants CTS-0338377 and NIRT-0403903. R.Y-R and I. S. are grateful to the BSF-United States-Israel Binational Science Foundation for supporting the cooperation leading to the development of the concepts presented in this work.

REFERENCES

1. M. S. Dresselhaus, G. Dresselhaus, and P. Avouris, *Carbon Nanotubes, Topics in Applied Physics* Vol (80), Berlin Heidelberg: Springer-Verlag (2001).
2. P. J. Harris, *Carbon Nanotubes and Related Structures, New Materials for the Twenty-first Century,* Cambridge: Cambridge University Press, (1999).
3. P. M Ajayan, J. C. Charlier, and A. G. Rinzler, *Proc. Nat. Acad. Sci.* 96, 14199 (1996).
4. R. H. Baughman, A. A. Zakhidov, and W. A. de Heer, *Science*, 297, 792 (2002).
5. P. G. Collins, and P. Avouris, *Scientific American* , December 62 (2002).
6. S. P. Frank, P. Poncharal, Z. L. Wang, and W. A. de Heer, *Science*. 280, 1744 (1998).
7. S. Iijima, *Nature* 354, 56 (1991).
8. S. Ijima and T. Ichihasui, *T. Nature* 363, 603 (1993).
9. A. Thess, R. Lee, P. Nikolaev, D. Hongjie, P. Petit, J. Robert, C. Xu, et al., *Science* 273, 483 (1996).
10. C. Journet W. K. Maser, P. Bernier, A. Loiseau, M. Lamydela, M. Chapelle, S. Lefrant, P. Deniard, R. Lee, and J. E. Fischer, *Nature* 388, 756 (1997).
11. A. G. Rinzler, J. Liu, H. Dai, P. Nikoleav, C. B. Huffman, F. Rodriguesz-Macias, P. J. Boul, et al., *Appl. Phys. A.* 67, 29 (1998).
12. S. J. Tans, A. R. M. Verschueren, and C. Dekker, *Nature* 393, 49 (1998).
13. W.A. de Heer, A. Chatelin, and D. Ugarte, *Science* 270, 1179 (1995).
14. V. Semet, V. T. Binh, P. Vincent, D. Guillot, K. B. K. Teo, M. Chhowalla, G. A. J Amaratunga, W. I. Milne, P. Legagneux, and D. Pribat, *Appl. Phys. Lett.* 81, 343 (2002).
15. *Chemical Sensors Science and Application of Nanotubes* D. Tománek and R. Enbody, eds. Kluwer Academic Publishers (2000).
16. J. G. Smith, J. W. Connell, D. M. Delozier, P. T. Lillehei, K. A. Watson, Y. Lin, B. Zhou, and Y. P. Sun, *Polymer* 45, 825 (2004).

17. M. R. Diehl, S. N. Yaliraki, R. A. Beckman, M. Barahona, and J. R. Heath, *Angew. Chem. Int. Ed.* 41, 354 (2002).
18. P. J. F. Harris, *International Materials Reviewes*, 49, 31 (2004).
19. O. Breuer and U. Sundararaj, *Polymer Composites,* 25, 630 (2004).
20. NASA, Johnson Space Center: The Nanomaterials Project http://mmptdpublic.jsc.nasa.gov/jscnano/.
21. C. Niu, E. K. Sichel, R. Hoch, D. Moy, and H. Tennent, *Appl. Phys. Lett.* 70, 1480 (1997).
22. J. Kong, N. R. Franklin, C. Zhou, M. G. Chapline, S. Peng, K. Cho, and H. Dai, *Science,* 287, 622–625 (2000).
AQ5 23. (a) SWNT synthesized via arc-discharge (Select grade, purity of 85 vol% Carbolex USA). Typical diameter = 1.3 nm typical length hundreds of nm (b) MWNT synthesized via arc-discharge (purity 40 vol%, ILJIN Nanotech Co., Ltd, Korea). Typical diameters 10–20 nm typical length 3–7 micron (c) SWNT synthesized via the HiPco process [25] (Carbon Nanotechnology Inc, USA). Typical diameter 1.2 nm and typical length of hundreds of nanometers to about 2 microns.
24. The images were taken by Dr. Yael Kalisman, The Ilze Katz Center for Meso and Nanoscale Science and Technology, Ben-Gurion University, Beer-Sheva Israel.
25. P. Nikolaev, M. J. Bronikowski, R. K. Bradley, F. Rohmund, D. T. Colbert, K. A. Smith, and R. E. Smalley, *Chem. Phys. Lett.* 313, 91 (1999).
26. P. M. Ajayan, L. S. Schadler, C. Giannaris, and A. Rubio, *Adv. Mater.* 12, 750 (2000).
27. I. Szleifer and R. Yerushalmi-Rozen, *Polymer* 46, 7803 (2005).
28. D. Tasis, N. Tagmatarchis, V. Georgakilas, and M. Prato, *Chem. Eur. J.* 9, 4000 (2003) and references therein.
29. J. Chen, M. A. Hamon, H. Hu, Y. Chen, A. M. Rao, P. C. Eklund, and R. C. Haddon, *Science* 282, 98 (1998).
30. J. Chen, A. M. Rao, S. Lyuksyutov, M. E. Itkis, M. A. Hamon, H. Hu, R. W. Cohn, et al., *Phys. Chem. B.* 105, 2525 (2001).
31. S. Niyogi, H. Hu, P. Bhowmik, B. Zhao, S. M. Rozenzhak, J. Chen, M. E. Ikis, et al., *J. Am. Chem. Soc.* 123, 733 (2001).
32. B. Zhao, H. Hu, S. Niyogi, M. E. Itkis, M. A. Hamon, P. Bhowmik, M. S. Meier, and R. C. Haddon, *J. Am. Chem. Soc.* 123, 11673 (2001).
33. Y. P. Sun, W. Huang, Y. Lin, K. Fu, A. Kitygorodskiy, L. A. Riddle, Y. J. Yu, and D. L. Carroll, *Chem. Mater.* 13, 2864 (2001).
34. K. Fu, W. Huang, Y. Lin, L. A. Riddle, D. L. Carroll, and Y. P. Sun, *Nano Lett.* 1, 439 (2001).
35. V. Cattien, P. Nguyen, L. Delzeit, A. M. Cassell, J. Li, J. Han, and M. Myyapen, *Nano Lett.* 2, 1079 (2002).
36. M. Shim, N. Wong, S. Kam, R. J. Chen, Y. Li, and H. Dai, *Nano Lett.* 4, 285 (2002).
37. H. Peng, L. B. Alemany, V. N. Khabashesku, and J. L. Margrave, *J. Am. Chem. Soc.* 125, 15174 (2003).
38. J. B. Baek, C. B. Lyons, and L. S. Tan, *J. Mater. Chem.* 14, 2052 (2004).
39. N. Nakashima, Y. Tomonari, and H. Murakami, *Chem. Lett.* 31, 638 (2002).
40. W. Zhm, N. Minami, S. Kazaoui, and J. Kim, *J. Mater. Chem.*
AQ6 1924 (2004).
41. B. Vigolo, A. Penicaud, C. Coulon, C. Sauder, R. Pailler, C. Journet, P. Bernier, and P. Poulin, *Science* 290, 1331 (2000).
42. M. J. O'Connell, S. M. Bachilo, C. B. Huffman, V. C. Moore, M. S. Strano, E. H. Haroz, K. L. Rialon, et al., *Science* 297, 593 (2002).
43. M. F. Islam, D. M. Rojs, A. T. Johnson, and A. G. Yodh, *Nano Lett.* 3, 269 (2003).
44. C. Richard, F. Balavoine, P. Schultz, T. W. Ebbesen, and C. Mioskowski, *Science* 300, 775 (2003).
45. O. Regev, E. L. Kati, J. Loos, and C. E. Koning, *Adv. Mater.* 16, 248 (2004).
46. J. Kono, G. N. Ostojic, S. Zaric, M. S. Strano, V. C. Moore, J. Shaver, R. H. Hauge, and R. E. Smalley, *Appl. Phys. A.* 78, 1093 (2004).
47. H. Wang, W. Zhou, D. L. Ho, K. I. Winey, J. E. Fischer, C. J. Glinka, and E. K. Hobbie, *Nano Lett.* 9, 1789 (2004).
48. J. N. Israelachvili, *Intermolecular and Surface Forces*, London: Academic Press, (1992).
49. L. A. Girifalco, M. Hodak, and R. S. Lee, *Phys. Rev. B*. 62, 13104 (2000).
50. U. S. Schwarz, S. Komura, and S. A. Safran, *Europhys. Lett.*, 50, 762 (2000).
51. R. Shvartzman-Cohen, E. Nativ-Roth, E. Baskaran, Y. Levi-Kalisman, I. Szleifer, and R. Yerushalmi-Rozen, *J. Am. Chem. Soc.* 126, 14850 (2004).
52. D. Costa, C. Caccamo, and M. C. Abramo, *J. Phys.: Cond. Matt.* 14, 2181 (2002).
53. L. A. Girifalco, *J. Phys. Chem.* 96, 858 (1992).
54. L. Jensen, P. O. Åstrand, and K. V. Mikkelsen, *J. Phys. Chem. A.* 108 (41), 8795 (2004).
55. U. S. Schwarz, and S. A. Safran, *Phys. Rev. E part B* 62, 6957 (2000).
56. M. het Panhuis, A. Maiti, A. B. Dalton, A. van den Noort, J. N. Coleman, B. McCarthy, and W. J. Blau, *J. Phys. Chem. B.* 107, 478 (2003).
57. V. C. Moore, M. S. Strano, E. H. Haroz, R. H. Hauge, R. E. Smalley, J. Schmidt, and Y. Talmon, *Nano Lett.* 3, 1379 (2003).
58. R. Shvartzman-Cohen, Y. Levi-Kalisman, E. Nativ-Roth, and R. Yerushalmi-Rozen, *Langmuir* 20, 6085 (2004).
59. R. Bandyopadhyaya, E. Nativ-Roth, O. Regev, and R. Yerushalmi-Rozen, *Nano Lett. 2,* 25 (2002).
60. R. Bandyopadhyaya, E. Nativ-Roth, O. Regev, and R. Yerushalmi-Rozen, *MRS Proceedings,* 706, 46303 (2002).
61. Napper, D. H. Eds, *Polymeric Stabilization of Colloidal Dispersions.* Orlando: FL: Academic Press, Inc., (1993).
62. Poly (styrene)-poly (methacrylic acid) di-block copolymer (PS-PMAA), where each PS block is of molecular weight 33,100 g/mol, and the PMAA block is of 6700 g/mol was purchased from Polymer Source Inc., Canada (P1861-SMAA, polydispersity index 1.1). AQ7
63. L. Liu, A. H. Barber, S. Nuriel, and D. H. Wagner, *Adv. Funct. Mater.* 15, 975 (2005).
64. N. Hadjichristidis, S. Pispas, and G. Floudas, *Block Copolymers: Synthetic Strategies, Physical Properties, and Applications* John Wiley & Sons Europe (2003).
65. A. Halperin, M. Tirell, and T. P. Lodge, *Adv. In Polymer Science* 100, 311 (1992).
66. D. Bedrov, C. Ayyagari, and G. D. Smit, *J. Chem. Theory Comput.* 2, 598-606 (2006).
67. D. Zhang, M. A. Carignano, R. Yerushalmi-Rozen, I. Szleifer, manuscript in preparation.
68. I. Szleifer and M. A. Carignano, *Adv. Chem. Phys.* 95, 165 (1996).
69. R. Nap and I. Szleifer, *J. Polym. Sci., Part B: Polym. Phys.* 44, 2638 (2006).
70. M. J. O'Connell, P. Boul, L. M. Ericson, C. Huffman, Y. Wang, E. Haroz, C. Kuper, J. Tour, K. D. Ausman, and R. E. Smalley, *Chem. Phys. Lett.* 342, 265 (2001).
71. T. Werder, J. H. Walther, R. L. Jaffe, T. Halicioglu F. Noca, and P. Koumoutskos, *Nano Lett.* 1, 12, 697 (2001).
72. Z. Guo, P. J. Sadler, and S. C. Tsang, *Adv. Mater.* 10, 701 (1998).
73. S. G. Chou, H. B. Ribeiro, E. B. Barros, A. P. Santos, D. Neizch, G. Samsonidze, C. Fantini, et al., *Chem. Phys. Lett*. 397, 296 (2004).
74. G. R. Dieckmann, A. B. Dalton, P. A. Johnson, J. Razal, J. Chen, G. M. Giordano, E. Munoz, I. H. Musselman, R. H. Baughman, and R. K. Draper, *J. Am. Chem. Soc.* 124, 1770 (2003).
75. M. Zheng, A. Jagota, E. D. Semke, B. A. Diner, R. S. Mclean, S. R. Lustig, R. E. Richardson, and N. G. Tassi, *Nature Materials* 2, 338 (2003).
76. O. P. Matyshevska, A. Y. Kavlash, Y. V. Shtogun, A. Benilov, Y. Kiryizov, K. O. Gorchinskyy, E. V. Bukaneva, Y. I. Prylutskyy, and P. Scharff, *Mater. Sci. Eng. C.* 15, 249 (2001).

77. J. N. Barisci, M. Tahhan, G. G. Wallace, S. Badaire, T. Vaugien, M. Maugey, and P. Poulin, *Adv. Func. Mate.* 14,133 (2004).
78. H. Gao, and Y. King, *Ann. Rev. Mater. Res.* 34, 13–50 (2004).
79. S. A. Curran, P. M. Ajayan, W. J. Blau, D. L. Carroll, J. N. Coleman, A. B. Dalton, A. P. Davey, A. Drury, B. McCarthy, and A. Strevens, *Adv. Mater.* 14, 1091 (1998).
80. S. Curran, A. P. Davey, J. N. Coleman, A. B. Dalton, B. McCarthy, S. Maier, A. Drury, et al., *Synth. Met.* 103, 2559 (1999).
81. N. Coleman, A. B. Dalton, S. Curran, A. Rubio, A. P. Davey, A. Drury, B. McCarthy, et al., *Advanced Materials* 12, 213 (2000).
82. Wu T-M, Lin Y-W, Liao C-S., *Carbon* 43,734 (2005) and references therein.
83. D. W. Schaefer, J. Zhao, D. P. Anderson, and D. Tomlin, *Chem. Phys. Lett.* 375, 369 (2003).
84. D. W. Schaefer, J. M. Brown, D. P. Anderson, J. Zhao, K. Chokalingam, and J. Ilavski, *J. Appl. Crystallogr.* 36, 553 (2003).
85. H. Wang, W. Zhou, D. L. Ho, K. I. Winey, J. E. Fischer, C. J. Glinka and E. K. Hobbie, *Nano Lett.* 4, 1789 (2004).
86. Y. Dror, W. Pyckhout-Hintzen, and Y. Cohen, *Macromolecules* 38, 7828 (2005).
87. Hye-in Shin, B. G. Min, W. Jeong, and C. Park, *Macromol. Rapid Commun.* 26, 1451, 1457 (2005).
88. Y. Kang, and T. A. Taton, *J. Am. Chem. Soc.* 125, 5650 (2003).
89. D. Stauffer, *Introduction to Percolation Theory* 1st ed. London: Taylor and Francis Ltd., (1985).
90. B. Vigolo, C. Coulon, M. Maugey, C. Zakri, and P. Poulin, *Science* 309, 920 (2005).
91. P. J. F. Harris, *International Materials Reviews* 491, 31 (2004).
92. J. C. Grunlan, A. R. Mehrabi, M. V. Bannon, and J. L. Bahr, *Adv Mater* 16, 150 (2004).
93. R. Ramasubramaniam, J. Chen, and H. Liu, *Appl Phys Lett.* 83, 2928 (2003).
94. M. A. Lopez-Manchado, J. Biagiotti, L. Valentini, and J. M. Kenny, *Journal of Applied Polymer Science* 92, 3394 (2004).
95. C. A. Mitchell, J. L. Bahr, S. Arepalli, J. M. Tour, and R. Krishnamoorti, *Macromolecules* 35, 8825 (2002).
96. E. D. Zhang, L. Shen, I. Y. Phang, and T. Liu, *Macromolecules* 37, 256 (2004).
97. A.V. Ruzette, and L. Leibler, Nature Materials 4, 19 (2005).
98. Gum arabic (GA) (Acacia 26,077-0) was purchased from Sigma-Aldrich, Israel, and used as received. 2) Pluronic P123 tri-block copolymer poly(ethylene oxide)-b-poly(propylene oxide)-b-poly (ethylene oxide), (PEO_{20}-PPO_{70}-PEO_{20}), (no. 583062), Mw = 5790 g/mol was obtained as a gift from BASF Corp. Germany and was used as received. Poly (ethyleneoxide-b-polydimethylsiloxane-b-ethyleneoxide) tri-block copolymer (PEO-PDMS-PEO), where each PEO block is of molecular weight 2000 g/mol, and the PDMS block is of 12 000 g/mol was synthesized by Y. Yagen. The matrix polymers were: Styrene-acrylate emulsion (Acronal 290D) purchased from BASF Corp. Germany, emulsion of acrylic polybutadiene copolymer Primal 928 purchased from Rhom and Hass, USA, and polydimethylsiloxane (PDMS) elastomer, together with a curing agent (Sylgard 184), purchased from Dow Corning Corporation, USA.
99. J. N. Coleman, *Phys. Rev. E,* 58, R7492 (1998).
100. S. P. Shaffer, and A. H. Windle, *Adv. Mater.* 11, 937 (1999).
101. P. Postschke, S. M. Dudkin, and L. Alig, *Polymer* 44, 5023 (2003).
102. J. M. Benoit, B. Carraze, and O. Chauvet, *Phys. Rev. B*. 65, 241405 (2003).
103. O. Breuer and U. Sundaaraj*, Polym. Composites,* 25, 630 (2004).
104. L. A. Hough, M. F. Islam, P. A. Janmey, and A. G. Yodth, *Phys Rev. Lett.* 93 168102 (2004).
105. M. Grujicic, G. Cao, and W. N. Roy, *Journal of Materials Science* 39, 4441 (2004).
106. H. R. Brown, *Materials Forum 2000,* 24, 49 http://www.mateng.asn.au/. AQ8

Author Queries

AQ1. Do the edits of this sentence correctly clarify your meaning?
AQ2. It should be mentioned that the attractive interactions between colloidal particles are proportional to the effective Hamaker constant. Therefore, by properly changing the medium where the particles are dispersed it is possible to achieve short-range attractive interactions for large colloidal particles. However, the presence of large vdW attractions with a range of a few times the particles size is the most common case [50, 55].
AQ3. Does this edit correctly clarify your meaning?
AQ4. The equation is not visible. Please provide the equation, and carefully check this sentence, as it is unclear as written.
AQ5. Please check to see if there is a reference that is missing here, or if the list should be renumbered and edit accordingly.
AQ6. Missing volume #, please insert.
AQ7. Are you wanting this to be cited in your reference list? Or is this misplaced? Please edit accordingly.
AQ8. web addresses require an accession date in the form of (Accessed month, year).
AQ9. For any figures that you may have borrowed from others' published works, please provide "Reprinted with permission from. . ." statements at the end of the figure caption.